NATIONAL ADVISORY COMMITTEE FOR AERONAUTICS

TECHNICAL NOTE 3430

ON SLENDER DELTA WINGS WITH LEADING-EDGE SEPARATION

By Clinton E. Brown and William H. Michael, Jr.

Langley Aeronautical Laboratory
Langley Field, Va.

Washington
April 1955

NATIONAL ADVISORY COMMITTEE FOR AERONAUTICS

TECHNICAL NOTE 3430

ON SLENDER DELTA WINGS WITH LEADING-EDGE SEPARATION

By Clinton E. Brown and William H. Michael, Jr.

SUMMARY

The slender-body approximation of linearized compressible flow is applied to the problem of a delta wing in which flow separation occurs at the leading edges. The vortex sheets found in the real flow are approximated by concentrated vortices with feeding lattices, and a plausible adaptation of Kelvin's theorem is applied to simulate the force-free nature of the vortex sheet.

The computations show that leading-edge separation produces an increase in lift over that given by the Jones slender-wing theory and that the lift does not vary linearly with angle of attack. Computed pressure distributions and span loadings are presented and the theoretical lift results are compared with the results of simple force tests made at a Mach number of 1.9.

INTRODUCTION

A large number of fluid flows are affected to the first order by the fluid viscosity and yet do not constitute motions having restrictive amounts of viscous dissipation. Such fluid flows may be treated as special cases of irrotational or potential flows; thus their simplification and ultimate solution are possible by well-known analytical methods. Kirchhoff (see ref. 1, p. 94) was probably the first to suggest this approach when he proposed that the drag of flat plates might be estimated by assuming that the flow separated from the sharp edges and formed a vortex wake behind the plate. Von Kármán (see ref. 1, p. 225) later calculated the asymptotic form of the wake also by assuming that the dissipation due to viscosity was small. There is little in the literature which concerns the details of separated flows; however, Prandtl (ref. 2) has discussed the formation of spiral vortex sheets at the edges of flat plates in two dimensions, and Anton (ref. 3) has computed the position of the spiral as a function of time for a plate suddenly set in motion. The emphasis of references 2 and 3 was primarily on the vortex behavior and no attempt was made to estimate the forces acting on the plate.

In the present paper, the flow over a slender delta wing is considered and leading-edge separation is assumed. The physical flow field over the wing is expected to look like the schematic drawing shown in figure 1(a), at least for vanishing aspect ratios; that is, separation occurs on the leading edge and produces the two spiral vortex sheets across which the pressure is continuous but the tangential velocity is discontinuous. For the slender delta wing in supersonic flow, the field is conical inasmuch as there is no characteristic dimension on which to base variations of any quantity along conical rays through the origin. Within the limits of slender-body theory, the model in figure 1(a) is also applicable to subsonic flows. The only contribution of viscosity in these flows is to fix the separation point at the leading edge for reasons exactly analogous to those justifying the use of the Kutta condition at subsonic trailing edges. Solution of the problem considering the spiral vortex sheet was found to be too difficult; hence, a simplified model, more amenable to calculation, was adopted. This model, shown in figure 1(b), replaces the spiral sheet with two concentrated line vortices above the wing and two feeding vortex sheets connecting the source of vorticity (leading edge) and the concentrated line vortices. It is expected that the results of the simplified-model calculations should give a fair estimate of the forces acting on the wing and indicate the important features of flows involving separated leading edges.

A paper by Legendre (ref. 4) dealing with the same problem has been discussed by Adams (ref. 5). Adams pointed out that Legendre's solution failed to account properly for the forces on the feeding vortex sheet and that inclusion of the sheet forces produced a result which in effect left an uncanceled finite force in the flow field over the wing. This difficulty was encountered by Dr. Adams and the senior author in a preliminary investigation of the problem, and acknowledgment is made to Dr. Adams for his contributions in the early stages of the work. In the present paper, the previously found difficulty is resolved by use of more appropriate boundary conditions. Clarification of this point is made in the analysis. Work of essentially the same result as the present report has also been discussed by Edwards in reference 6.

Experiments are described which allow comparison of the theoretically predicted forces with the test results, and a discussion is given of some factors affecting the overall problem of leading-edge separation on sweptback wings. The essential theoretical work reported herein was presented in a more condensed form in reference 7.

SYMBOLS

a	half-wing span at any chordwise station x
C_L	lift coefficient, $\frac{L}{\frac{\rho V^2}{2}(\text{Wing area})}$
L	lift
M	Mach number
m	apparent mass
p	pressure
$\Delta p/q = \frac{p_{local} - p_{free\ stream}}{\frac{1}{2}\rho V^2}$	
V	free-stream velocity
v,w	disturbance velocities in y- and z-directions, respectively
v^*	mean normal flow velocity over vortex
W	complex velocity potential
x	coordinate along wing in direction of free stream
y	coordinate along wing normal to free stream
z	coordinate normal to wing surface
α	angle of attack
Γ	vortex-core strength
ϵ	semivertex angle of wing
η	imaginary part of θ
θ	vector-point coordinate (see fig. 2), $\xi + i\eta$
$\bar{\theta}$	complex conjugate of θ, $\xi - i\eta$

ξ real part of θ

ρ free-stream density

σ vector-point coordinate (see fig. 2), $y + iz$

$\bar{\sigma}$ complex conjugate of σ, $y - iz$

φ disturbance velocity potential

Subscripts:

o value at vortex position

1 flow condition with right vortex removed

Partial differentiation is indicated by subscripts; that is, $\varphi_{xx} = \frac{\partial^2 \varphi}{\partial x^2}$.

ANALYSIS

Computation of Flow Field

The problem to be considered is that of potential flow about a slender delta wing on which leading-edge separation exists; that is, the streamlines of the flow which wet the wing do not pass from the lower to the upper surface but rather come from both surfaces and leave at the leading edge. In reality, such a condition would produce a conical spiral vortex sheet above the wing, and the boundary conditions of the problem would be that no fluid pass through the wing surface and that the pressure across the vortex sheet be continuous. Clearly this situation represents a difficult problem because the solution must provide both the shape and strength of the sheet. Past experience with vortex sheets leads to the hope that the main features of the flow can be obtained by replacing the spiral sheet by a concentrated vortex near the center of the spiral. For conical flow, however, the net vorticity in the spiral is linearly increasing in the downstream direction; hence, the concentrated vortex must also be of linearly increasing strength. The increase in strength must be accomplished by a feeding vortex sheet in order to satisfy Kelvin's theorem; thus, the model shown in figure 1(b) seems to be the most appropriate flow field amenable to simple calculation.

The equation of motion to be satisfied represents a slightly perturbed main stream of velocity V and corresponding Mach number M:

$$\left(1 - M^2\right)\varphi_{xx} + \varphi_{yy} + \varphi_{zz} = 0 \qquad (1)$$

where φ is the disturbance velocity potential and x, y, and z are Cartesian coordinates fixed to the wing. (The coordinate z is measured perpendicular to the flat wing surface, y is tangential to the wing surface but normal to the free-stream velocity vector, and x is measured in the flow direction along the wing.) If the flow is further restricted to highly swept wings, the term $(1 - M^2)\varphi_{xx}$ may be neglected and the equation of motion becomes Laplace's equation in y and z:

$$\varphi_{yy} + \varphi_{zz} = 0 \tag{2}$$

With this assumption, the well-known slender-body theory can be used; hence, subsequent discussion will generally be related to the two-dimensional flow field.

Boundary conditions.- The boundary conditions at the plate are that the plate is solid and hence the normal velocities are zero and that the flow separates tangentially at the plate edges. The boundary conditions in the field are that the disturbances vanish at infinity and that the fluid pressure is continuous. In the real flow the last condition is satisfied by the fact that vortex elements lie along streamlines. The last condition is, however, impossible to satisfy with the assumed model and hence must be replaced with one which is more compatible. The difficulty lies in the presence of the feeding vortex sheet across which a pressure discontinuity must exist (because there is a component of the velocity through the sheet), but since the assumed vortex system represents the true spiral only at a distance, it is to be expected that, in the small regions near the system, violation of natural conditions might occur. It is, therefore, necessary to make the last boundary condition less detailed and hence to require only that the integral of pressure around the assumed vortex system vanish. In simpler terms, as a final condition the assumed vortex system (feeding sheet and concentrated vortex) must have zero net force acting since only the wing and not the fluid can sustain forces. Application of this idea to the model then requires that the forces on the feeding vortex sheet be cancelled by equal but opposite forces on the concentrated vortex; thus the concentrated vortex is not force free as was assumed in the Legendre solution (ref. 4). The mathematical formulation of the preceding boundary condition is as follows: At a given station x where the half-wing span is a, introduce the quantity $\sigma = y + iz$, the vector distance to a point (y,z). The feeding sheet is assumed to be composed of filaments stretching from the leading edge to the vortex core as shown in figure 1(b). The vector force on each filament representing the vorticity lying between x and a point $x + dx$ can be expressed as

$$i\rho V \frac{d\Gamma}{dx}(\sigma_o - a)$$

because Γ, the vortex-core strength, is a linearly increasing function of x and hence $\frac{d\Gamma}{dx}$ is constant for all values of x. (Note that cosines of small angles are taken equal to unity.) The vector force on the concentrated vortex must be produced by a fluid flow normal to the vortex and of vector velocity v^*. The vector force would be

$$-i\rho v^*\Gamma$$

Setting the vector sum of the two forces equal to zero in accordance with the previous discussion thus yields

$$v^* = V \frac{d\Gamma}{dx} \frac{\sigma_o - a}{\Gamma} = V\epsilon \frac{\sigma_o - a}{a} \tag{3}$$

where $\epsilon = \frac{a}{x}$ and $\Gamma = x \frac{d\Gamma}{dx}$ because the vortex strength is linear in x. Equation (3) thus requires that the resultant flow velocity normal to the concentrated vortex filament be a function of the vortex position and the wing semivertex angle ϵ. The complex velocity v^* is, however, produced by the component of the main stream normal to the concentrated vortex plus the normal component of the velocity due to the disturbance velocity potential φ. The disturbance velocity is singular at the vortex position; however, v^* can be expressed as

$$v^* = -V\epsilon \frac{\sigma_o}{a} + (v + iw)_{1_{\sigma=\sigma_o}} \tag{4}$$

and hence,

$$(v + iw)_{1_{\sigma=\sigma_o}} = V\epsilon\left(\frac{2\sigma_o}{a} - 1\right) \tag{5}$$

where the velocity $(v + iw)_1$ evaluated at $\sigma = \sigma_o$ represents the average stream velocity over the vortex position and is easily computed in the usual manner by subtracting the velocity field of the vortex (purely circulatory about σ_o) from the complex velocity and then by taking the limit as σ approaches σ_o.

Potential solution.- A solution of equation (2) is now sought which satisfies the aforementioned boundary conditions. The unknowns in the problem are the location and strength of the concentrated vortex and the lift on the plate. The complex velocity potential $W(\sigma,a)$ is now introduced and is composed of the sum $\varphi + i\psi$ where ψ is a function similar to a stream function but has no physical significance with respect to the three-dimensional streamlines of the flow. The

dependence of the solution on x lies only in the relationship between x and a because, according to the slender-body concept, a gradual longitudinal deviation from a two-dimensional flow pattern changes the crossflow velocity field negligibly. For the same reason, the transverse vorticity on the wing and in the feeding vortex sheet does not contribute to the complex potential function in the crossflow plane. The solution of interest is derived by conformal mapping of the flow past two symmetrically placed vortices of equal but opposite strength. Thus, in the θ-plane (see fig. 2)

$$W(\theta) = -\frac{i\Gamma}{2\pi} \log_e \frac{\theta - \theta_o}{\theta + \bar{\theta}_o} - iV\alpha\theta \tag{6}$$

Transforming equation (6) to the σ-plane by the substitution $\theta = \sqrt{\sigma^2 - a^2}$ yields

$$W(\sigma) = -\frac{i\Gamma}{2\pi} \log_e \frac{\sqrt{\sigma^2 - a^2} - \sqrt{\sigma_o^2 - a^2}}{\sqrt{\sigma^2 - a^2} + \sqrt{\bar{\sigma}_o^2 - a^2}} - iV\alpha\sqrt{\sigma^2 - a^2} \tag{7}$$

Equation (7), which was also given by Riabouchinsky (see ref. 8, p. 254), thus represents the flow normal to an impermeable flat plate having two symmetrically placed vortices of equal but opposite strengths located at positions σ_o and $-\bar{\sigma}_o$.

The boundary condition that the flow leave the plate tangentially at the edges yields the following relationship between Γ and $V\alpha$:

$$\frac{2\pi V\alpha}{\Gamma} = \frac{1}{\sqrt{\sigma_o^2 - a^2}} + \frac{1}{\sqrt{\bar{\sigma}_o^2 - a^2}} \tag{8}$$

This equation is easily obtained in the θ-plane by requiring the presence of a stagnation point at the origin.

The final boundary condition to be applied (eq. (5)) requires the calculation of the mean velocity at the vortex location; hence, the effect of the complex function $W(\sigma)$ less the complex potential function of the right-hand vortex must be considered, or

$$W_1(\sigma) = W(\sigma) + \frac{i\Gamma}{2\pi} \log_e(\sigma - \sigma_o) \tag{9}$$

Differentiating equation (9) with respect to σ and setting σ equal to σ_o yields the conjugate of the complex velocity, or $(v - iw)_1$, at the vortex location.

Rearranging real and imaginary parts of equation (5) yields

$$(v - iw)_{1\sigma=\sigma_o} = V\epsilon\left(\frac{2\bar{\sigma}_o}{a} - 1\right) \tag{10}$$

and combining equations (7) to (10) results in

$$\frac{i\Gamma}{2\pi}\left[\frac{\sigma_o}{\sigma_o^2 - a^2 + \sqrt{\left(\sigma_o^2 - a^2\right)\left(\bar{\sigma}_o^2 - a^2\right)}} - \frac{\sigma_o}{\sqrt{\left(\sigma_o^2 - a^2\right)\left(\bar{\sigma}_o^2 - a^2\right)}} - \frac{\sigma_o}{\sigma_o^2 - a^2} + \frac{1}{2}\frac{a^2}{\sigma_o\left(\sigma_o^2 - a^2\right)}\right] = V\epsilon\left(\frac{2\bar{\sigma}_o}{a} - 1\right) \tag{11}$$

Equation (11) gives the means of finding the vortex location σ_o because the real and imaginary parts give two equations in the unknown coordinates y_o and z_o. Upon separation of equation (11) into its real and imaginary parts, the simultaneous equations were found to be greatly expanded and not amenable to analytic solution. Consequently, the equations were solved in a numerical manner by choosing a value of z_o and finding the value y_o which would give an equal value of the common parameter $\Gamma/V\epsilon$ for the two equations. Equation (11) was also solved approximately by assuming the absolute value of σ_o to be nearly equal to a and expanding the radicals in power series. A solution was thus obtained which was valid to the second order in the parameter $\frac{\sigma_o - a}{a}$. This simplified approach gives an analytic expression for the position of the vortex which is

$$\frac{y_o - a}{a} = \frac{1}{2}\left(\frac{z_o}{a}\right)^{2/3}\left[1 - \frac{3}{4}\left(\frac{z_o}{a}\right)^{2/3}\right] \tag{12}$$

The approximate solution is plotted, together with the exact solution of equation (11), in figure 3. It is seen that the path of the vortex center of gravity moves inboard and up as is already known to be the correct physical motion, and the center of vorticity appears to become asymptotic to a vertical line at about 84 percent of the semispan. The agreement between the approximate and exact solutions is excellent.

The variations of both vortex position and vortex strength with angle of attack were obtained by making use of the relationship between z_o and y_o and equations (8) and (11). These computations were performed both approximately and exactly, and the results are given in

figures 4 and 5. The approximate equations governing the angle of attack and vortex strength are

$$\frac{\alpha}{\epsilon} = 4\,\frac{z_o}{a}\left[1 + \frac{1}{2}\left(\frac{z_o}{a}\right)^{2/3}\right] \tag{13}$$

and

$$\frac{\Gamma}{2\pi a V \epsilon} = \frac{1}{2}\left[1 + \frac{3}{2}\left(\frac{z_o}{a}\right)^{2/3}\right]\frac{\alpha}{\epsilon} \tag{14}$$

For small angles of attack the vortex cores lie in a plane inclined to the free stream at an angle three-fourths the angle of attack of the plate, and hence the vertical position of the cores is almost a linear function of the angle of attack. Figure 5 indicates that the vortex strength increases roughly linearly with angle of attack.

Computation of Lift and Pressure Distribution

Lift results.- The lift is most easily obtained from momentum considerations or by computing the flow of downward momentum through an infinite plane perpendicular to the stream at the trailing edge; thus,

$$L = -\rho V \iint \left(\varphi_z - V\alpha\right) dz\, dy = -\rho V \int_C \varphi\, dy \tag{15}$$

Here the contour is the wing trace plus the cuts connecting the wing tips and the vortex center. Note that φ_z is the velocity component in a plane perpendicular to the wing surface and hence contains, in the present usage, the upwash contribution of the main stream.

Equation (15) can be expressed in terms of the complex potential $W(\sigma)$ because $W(\sigma) = \varphi + i\psi$ as

$$L = \text{R.P.}\left[-\rho V\left(\int_C W\, d\sigma + \int_C \psi\, dz\right)\right] \tag{16}$$

where R.P. stands for the real part of the complex function. The integration of ψ is zero around the closed curve since ψ is single valued in the field and constant on the wing boundary. Furthermore, the function $W(\sigma)$ is analytic in the field external to the contour; hence, the integral is independent of the path provided that it encloses the original contour.

The simplest integration is obtained by transforming equation (16) to the θ-plane; hence,

$$L = -\text{R.P.}\left[\rho V \int_C W(\theta)\frac{d\sigma}{d\theta}\,d\theta\right] \tag{17}$$

Substituting equation (6) gives

$$L = \text{R.P.}\left[i\rho V \int_C \left(\frac{\Gamma}{2\pi}\log_e\frac{\theta - \theta_o}{\theta + \bar{\theta}_o} + V\alpha\theta\right)\left(\frac{\theta}{\sqrt{\theta^2 + a^2}}\right)d\theta\right]$$

$$= \rho V\Gamma\left(\theta_o + \bar{\theta}_o\right) + \rho V^2\alpha\pi a^2 \tag{18}$$

or, in lift-coefficient form,

$$C_L = \frac{2\Gamma\epsilon}{Va}\,\frac{\theta_o + \bar{\theta}_o}{a} + 2\pi\alpha\epsilon \tag{19}$$

In this equation, the second term represents the lift which would be obtained in the absence of leading-edge separation (the lift as computed by Jones, ref. 9), and the first term represents the departure from the Jones value. The real function $\frac{\theta_o + \bar{\theta}_o}{a}$ is a function of α/ϵ, and Γ is proportional to $aV\alpha$ times a function of α/ϵ; hence, the lift coefficient may be expressed as $\alpha\epsilon f(\alpha/\epsilon)$ or its equivalent, $\epsilon^2 f(\alpha/\epsilon)$. The lift computations for all aspect ratios can therefore be given by a single curve which is presented in figure 6 for the exact solution of equation (19) along with two approximations thereof. The curve labeled "First order" was also obtained by Edwards in reference 6 and is computed as mentioned in the previous section by expanding the equations in series form about the wing tip and retaining only first-order terms in $\frac{\sigma - a}{a}$. The second-order result is obtained by extending the analysis to include terms of the next highest order. In view of the obvious approximations involved in the fundamental assumptions of the theory, the small differences indicated in figure 6 are probably of little consequence. The analytical expression for the second-order result is

$$\frac{C_L}{\epsilon^2} = \frac{2\pi\alpha}{\epsilon} + 16\pi\left(\frac{\alpha}{4\epsilon}\right)^{5/3}\left[1 + \frac{2}{3}\left(\frac{\alpha}{4\epsilon}\right)^{2/3}\right] \tag{20}$$

The Jones results are also included in figure 6 for comparative purposes.

The calculations predict an increased lift when leading-edge separation is present. This result can be shown to hold true for the case in which the full spiral sheet is treated, and the Jones result representing a crossflow of minimum kinetic energy also represents the minimum lift or minimum crossflow apparent mass. The lift and apparent mass are directly related according to Munk (ref. 10) and can be expressed by the equation

$$L = V^2 \alpha m$$

where m is the additional apparent mass of the flow field in a plane perpendicular to the main stream at the trailing edge of the wing. The proof of the minimum-lift theory is given in the appendix.

Pressure distribution.- The first-order expression for the pressure coefficient is

$$\frac{\Delta p}{q} = \left(-2 \frac{\varphi_x}{V} + \alpha^2 - \frac{\varphi_y^2}{V^2} \right)_{z=0} \tag{21}$$

on the wing surface. The second term on the right does not normally arise when coordinates fixed with respect to the free stream are used; however, it is necessary when the coordinates are tilted through an angle of attack, as is the case in the present analysis. This term does not contribute to the lift. The factor φ_x can be expressed as $\varphi_a \frac{da}{dx}$ where $\frac{da}{dx} = \epsilon$, the semivertex angle. The velocity potentials appearing in equation (21) can be obtained from the complex potential function of equation (7) by differentiation and by using the definitions

$$\varphi_y = \text{R.P.} \frac{\partial w}{\partial \sigma}$$

and

$$\varphi_a = \text{R.P.} \frac{\partial w}{\partial a}$$

Therefore the pressure coefficient becomes

$$\frac{\Delta p}{q} = -\frac{2\epsilon}{V} \left(\frac{\partial w}{\partial a} \right)_{z=0} + \alpha^2 - \frac{1}{V^2} \left(\frac{\partial w}{\partial \sigma} \right)^2_{z=0} \tag{22}$$

Pressure distributions were calculated for a 15° semivertex-angle wing, and the results are plotted in figure 7. Results for other aspect ratios can be easily obtained since, for any given value of α/ϵ, both

lift and pressure distributions are proportional to ϵ^2. The very-low-pressure region on the wing upper surface is caused by the presence of the vortex, and the negative pressure peak corresponds approximately to the lateral position of the vortex.

Figure 8 shows the corresponding span loadings which are of interest in that a considerable deviation from the elliptical loading can be seen.

GENERAL PHYSICAL CONSIDERATIONS

The present theory should be considered a limiting one for vanishingly small values of the aspect ratio; hence, its primary usefulness is to give a better picture of what a real flow does in such a limiting case. When finite aspect ratios are contemplated, several important physical modifications arise. One of these modifications is evident from the pressure distributions (fig. 7) where, for $\epsilon = 15^\circ$, the upper-surface absolute pressure is calculated to be negative even for moderate Mach numbers. Clearly then, compressibility effects must modify those flow patterns, pressure distributions, and span loadings considerably when the pressures approach the vacuum condition. Just how the modification occurs is not fully known; however, in some cases experiments have shown two distinct types of leading-edge behavior (ref. 11), one separated and the other unseparated, with a special shock system replacing the vortex sheet.

Another physical modification which can occur is the breaking-up of the spiral vortex sheet into two or more spirals or regions of concentrated vorticity. The occurrence of such a pattern is dependent on the stability of the vortex sheet formed at the wing leading edge. Testing the three-dimensional sheet for reaction to small disturbances is an extremely difficult problem, and even its two-dimensional counterpart, the formation of a Kármán street behind an impulsively started flat plate, has not been solved. Finally, a pressure gradient which is conducive to boundary-layer separation appears to be situated near the leading edge of the triangular wing with separated flow. In such a situation, a secondary vortex having a rotational direction opposite that of the main sheet would be produced; hence, a modification of the assumed physical-flow picture would result. (The existence of such a vortex was first pointed out to the authors by Professor N. Rott of Cornell University.) In the latter case, the presence of secondary separation should be dictated by the pressure gradients normal to the leading edge on the upper surface; hence, for wings with finite angles at the edge, a crossflow stagnation point should exist and the separation tendency should be more pronounced than on a flat plate or a cusped-leading-edge profile.

Of some interest in the present theory are the stream surfaces in the three-dimensional flow. Clearly, the streamlines leaving the leading edge curl up into the center of the vortex spiral; however, one adjacent streamline passes over the spiral, impinges on the upper surface or plane of symmetry, and splits into two parts, one part passing almost straight backward on the upper wing surface and the other part passing into the vortex-spiral region to form the inner side of the vortex spiral. Such streamlines form a conical stream sheet which, when intersected by a plane perpendicular to the free-stream velocity, looks like the sketches of figure 9. The surface ray along which the flow impinges has been calculated for the simplified model and the results are given in figure 9. As the angle of attack increases, the impingement point moves inboard from the leading edge until, at a value of $\frac{\alpha}{\epsilon} \approx 1$, it moves onto the plane of symmetry.

EXPERIMENTS

Lift and pitching-moment data were obtained on three wings with semivertex angles of 5°, 7.5°, and 10° in a Mach number 1.9 blowdown jet of the Langley gas dynamics laboratory. The wings had sharp 1° wedge airfoil sections with 9-inch root chords and were semispan models mounted on a boundary-layer scoop-off plate, the leading edge of which was $1\frac{3}{8}$ inches forward of the wing apex. Although the wings were mounted on the scoop-off plate, a boundary layer with a thickness of 3 percent of the semispan of the smallest wing still existed. From unpublished data, the effect of this boundary layer on the lift results is believed to be negligible. Forces and moments were obtained from a strain-gage balance system and tests were conducted at a Reynolds number level of 1.6×10^6 per inch.

The experimental lift data are compared with the Jones slender-wing theory in figure 10. The data exhibit the same nonlinearity as predicted but fall progressively lower than the theoretical curve as the apex angle is increased. Compressibility effects as discussed in a previous section are believed to account for the decrease in actual lift over that predicted theoretically. Inasmuch as the compressibility effects should become less important with decrease in ϵ or Mach number, the present tests at a constant Mach number of 1.9 should indicate a decrease in compressibility effects with smaller values of ϵ. This is apparently what happens, since the predicted and measured values tend to converge as ϵ approaches zero.

Drag-due-to-lift results are not presented for these flat wings because the drag equals the lift times the angle of attack since there

is no leading-edge suction. The lack of leading-edge suction in the theory results directly from the application of the Kutta condition at the leading edge; hence, the edge velocities and pressures are required to be finite. The center of pressure is located at the two-thirds-root-chord position, as would be expected for any conical flow.

CONCLUSIONS

An approximate theory for the flow over delta wings having separated flow at their leading edges leads to the following conclusions:

1. The lift-curve slope of wings of low aspect ratio should be nonlinear and higher than the lift-curve slope obtained from slender-wing theory in which leading-edge separation was not assumed. For the higher aspect ratios (apex angles), little change in lift-curve slope should be expected for the two cases.

2. The span load distribution and wing pressure distribution are markedly affected by the presence of leading-edge separation.

3. Experimental force measurements on very slender delta wings having semivertex angles of 5°, 7.5°, and 10° at a Mach number of 1.9 indicate good agreement between theory and experiment for the most slender wing with gradually increasing discrepancies as the apex angle was increased. The data are as yet insufficient to show whether the fundamental assumptions of the theory are satisfied.

Langley Aeronautical Laboratory,
National Advisory Committee for Aeronautics,
Langley Field, Va., January 14, 1955.

APPENDIX

CALCULATION OF MINIMUM LIFT OF DELTA WINGS

The complete problem of the wing with a spiral vortex sheet is at present unsolved; however, certain limiting values of the lift may be established from fundamental considerations. For the continuous-spiral-sheet problem, the lift may be written as (eq. (17))

$$L = -R.P.\left[\rho V \int_C W(\theta)\, \frac{d\sigma}{d\theta}\, d\theta\right] \tag{A1}$$

where $W(\theta)$ now represents the complex potential function and may be considered to be made up of two parts: one, the Jones solution (ref. 9), or that corresponding to irrotational motion of the fluid about the flat plate; and the other, the contribution of the spiral vortex sheet. The first part gives the lift $\rho V^2 \alpha \pi a^2$ as in equation (18); the second gives the lift increment $\rho V \frac{d\Gamma}{d\tau}\left(\theta_o^* + \bar{\theta}_o^*\right)d\tau$ for each segment $d\tau$ of the vortex sheet, where $\theta_o^* + \bar{\theta}_o^*$ is the lateral distance from the imaginary axis to a point on the vortex sheet and τ is a distance measured along the sheet. The lift contributed by the vortex sheet is thus

$$\rho V \int \frac{d\Gamma}{d\tau}\left(\theta_o^* + \bar{\theta}_o\right)d\tau \tag{A2}$$

where the integration is performed along the sheet from the origin to the center of the spiral.

The boundary condition requires that the flow separate tangent to the plate edges. In the θ-plane this condition is equivalent to requiring a stagnation point at the origin. Thus, the boundary condition in the θ-plane can be written as

$$\left[\frac{dW(\theta)}{d\theta}\right]_{\theta \longrightarrow 0} = 0 \tag{A3}$$

or, in detail, the velocity contribution from the spiral vortex sheet must oppose the velocity of the motion at the origin and, hence, must equal $-V\alpha$. If these conditions are expressed in terms of the vortex elements of the sheet,

$$\int \frac{d\Gamma}{d\tau}\, \frac{\theta_o^* + \bar{\theta}_o^*}{R^2}\, d\tau = \frac{1}{2} V\alpha \tag{A4}$$

where R is the distance between a point on the sheet and the origin and, as in equation (A2), the integration extends over the length of the spiral sheet.

By comparing equations (A2) and (A4) it can be seen that, if $\frac{d\Gamma}{d\tau}$ is of like sign everywhere, the lift contribution of the vortex system must be positive. However, the sign of $\frac{d\Gamma}{d\tau}$ must be always the same because, in the conical flow, vorticity is generated uniformly at the leading edge of the wing and the vortex filaments pass back and into the spiral and change only their lateral spacing $\left(\text{and the magnitude of } \frac{d\Gamma}{d\tau}\right)$ but never cross and thus never change sign. It is proved then that, for the conditions stated, the vortex spiral contributes only positive lift over that contributed by the irrotational-flow (Jones) solution. Hence, the Jones lift result is the lower limit of lift for the complete spiral problem as well as for the approximation of the present report.

REFERENCES

1. Lamb, Horace: Hydrodynamics. Sixth ed., Cambridge Univ. Press, 1932, pp. 94 and 225.

2. Prandtl, L.: Über die Entstehung von Wirbeln in der idealen Flüssigkeit, mit Anwendung auf die Tragflügeltheorie und andere Aufgaben. Vorträge aus dem Gebiete der Hydro- und Aerodynamik (Innsbruck), 1922, pp. 18-33.

3. Anton, Leo.: Ausbildung eines Wirbels an der Kante einer Platte. Ing.-Archiv, Bd. X, Heft 6, Dec. 1939, pp. 411-427.

4. Legendre, Robert: Écoulement au voisinage de la pointe avant d'une aile à forte flèche aux incidences moyennes. La Recherche Aéronautique (O.N.E.R.A.), No. 30, Nov.-Dec. 1952, pp. 3-8; No. 31, Jan.-Feb. 1953, pp. 3-6.

5. Adams, Mac C.: Leading-Edge Separation From Delta Wings at Supersonic Speeds. Jour. Aero. Sci. (Readers' Forum), vol. 20, no. 6, June 1953, p. 430.

6. Edwards, R. H.: Leading-Edge Separation From Delta Wings. Jour. Aero. Sci. (Readers' Forum), vol. 21, no. 2, Feb. 1954, pp. 134-135.

7. Brown, C. E., and Michael, W. H., Jr.: Effect of Leading-Edge Separation on the Lift of a Delta Wing. Jour. Aero. Sci., vol. 21, no. 10, Oct. 1954, pp. 690-694 and 706.

8. Bateman, H.: Partial Differential Equations of Mathematical Physics. American ed., Dover Publications, 1944, p. 254.

9. Jones, Robert T.: Properties of Low-Aspect-Ratio Pointed Wings at Speeds Below and Above the Speed of Sound. NACA Rep. 835, 1946. (Supersedes NACA TN 1032.)

10. Munk, Max M.: The Aerodynamic Forces on Airship Hulls. NACA Rep. 184, 1924.

11. Lindsey, W. F., Daley, Bernard N., and Humphreys, Milton D.: The Flow and Force Characteristics of Supersonic Airfoils at High Subsonic Speeds. NACA TN 1211, 1947.

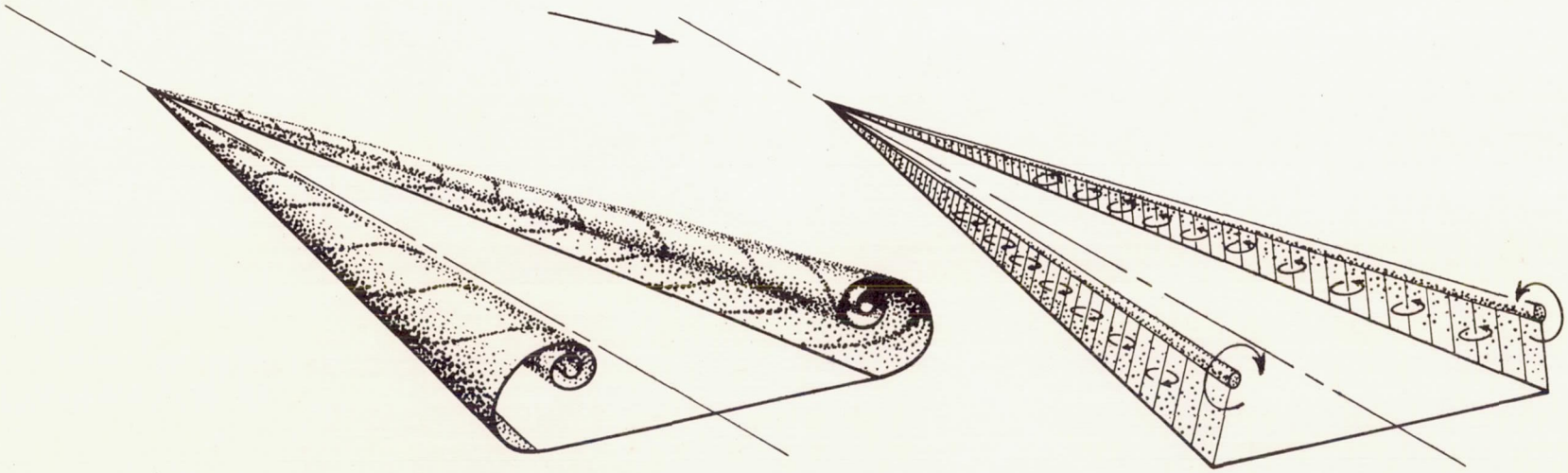

(a) Assumed flow field.

(b) Approximated flow field.

Figure 1.- Schematic drawings of separated flow over slender delta wings.

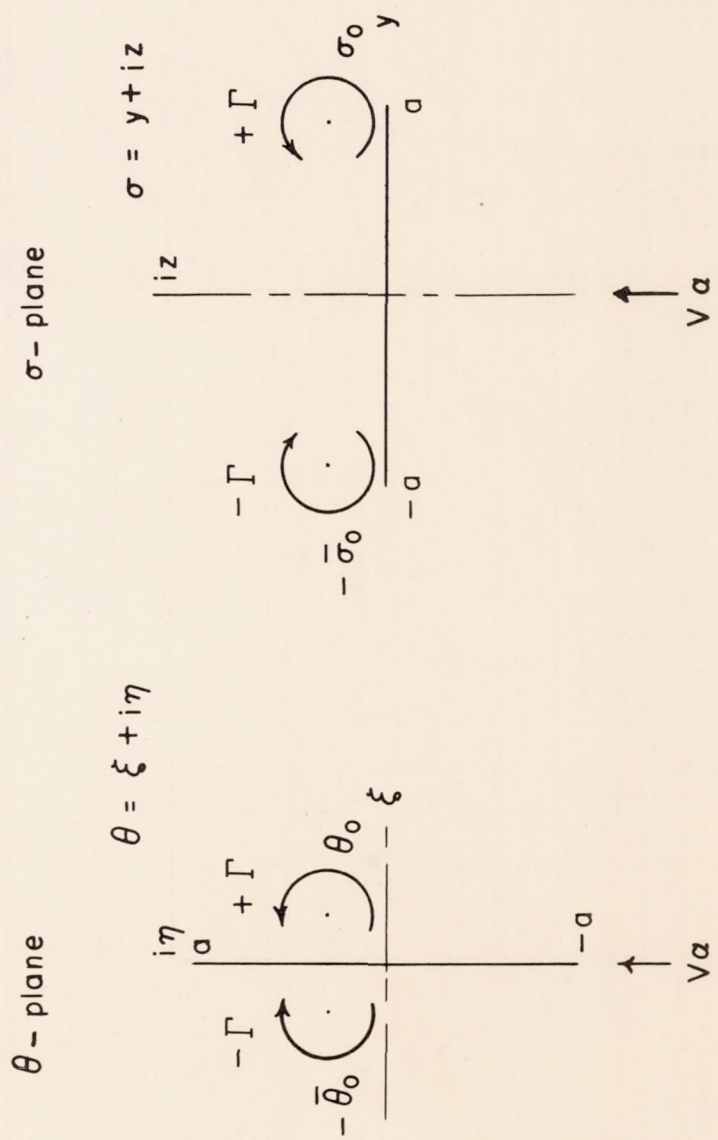

Figure 2.- Coordinate axes and symbol notations.

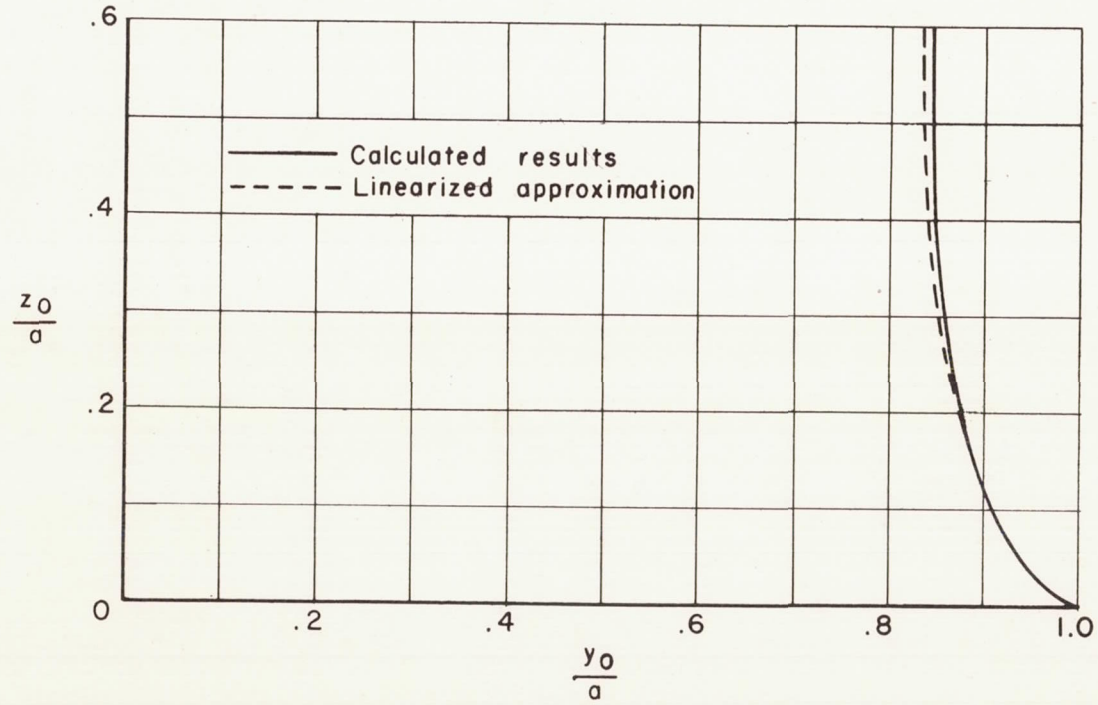

Figure 3.- Vortex positions.

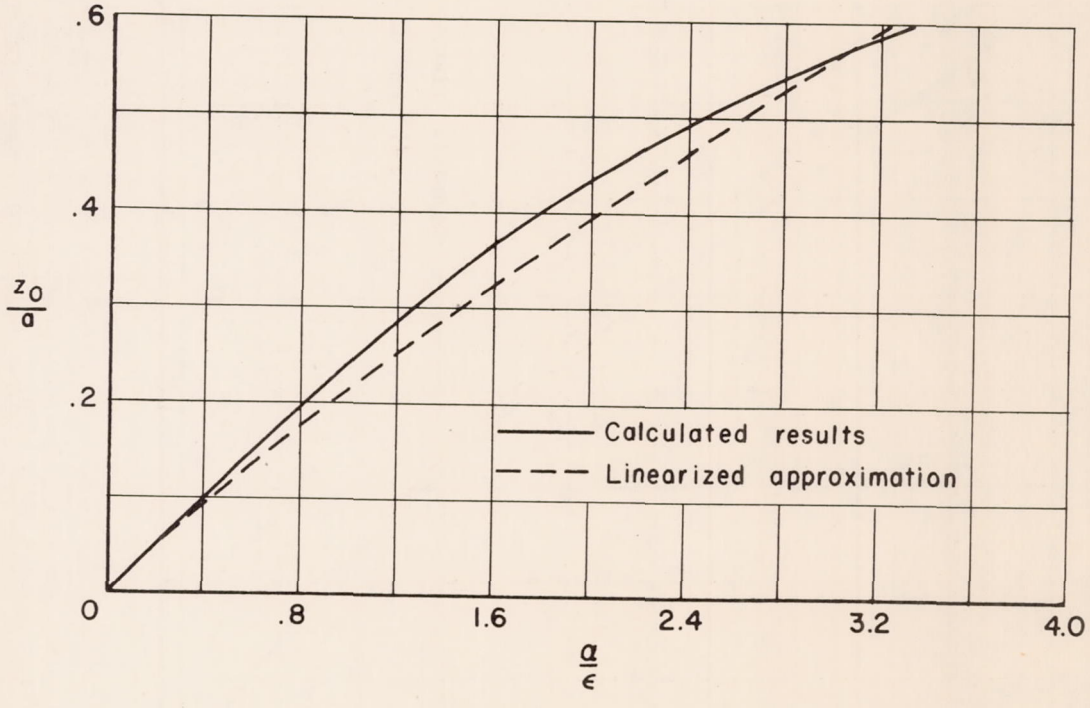

Figure 4.- Relation between vortex positions and angle of attack.

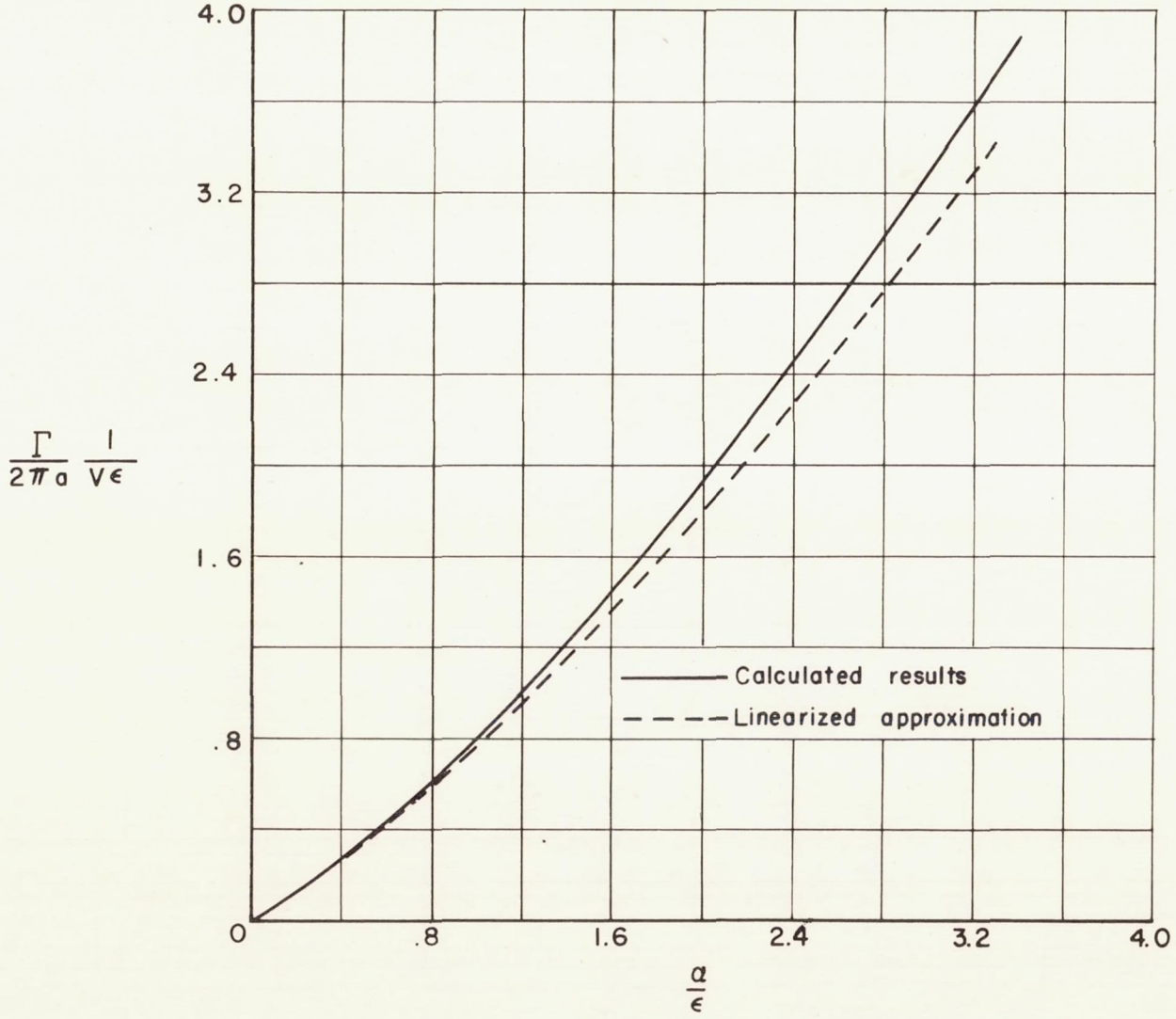

Figure 5.- Relation between vortex strength and angle of attack.

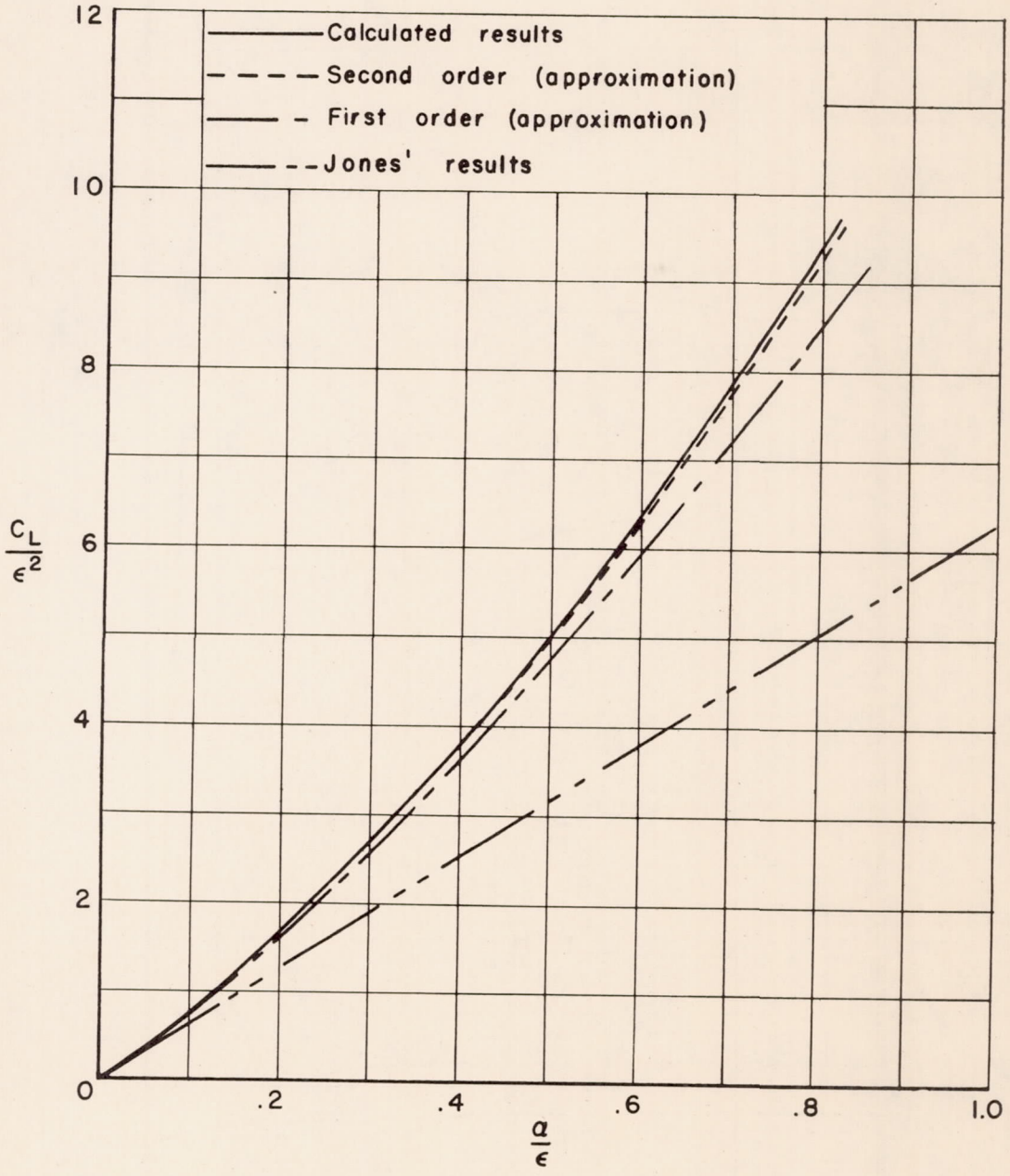

Figure 6.- Calculated lift results.

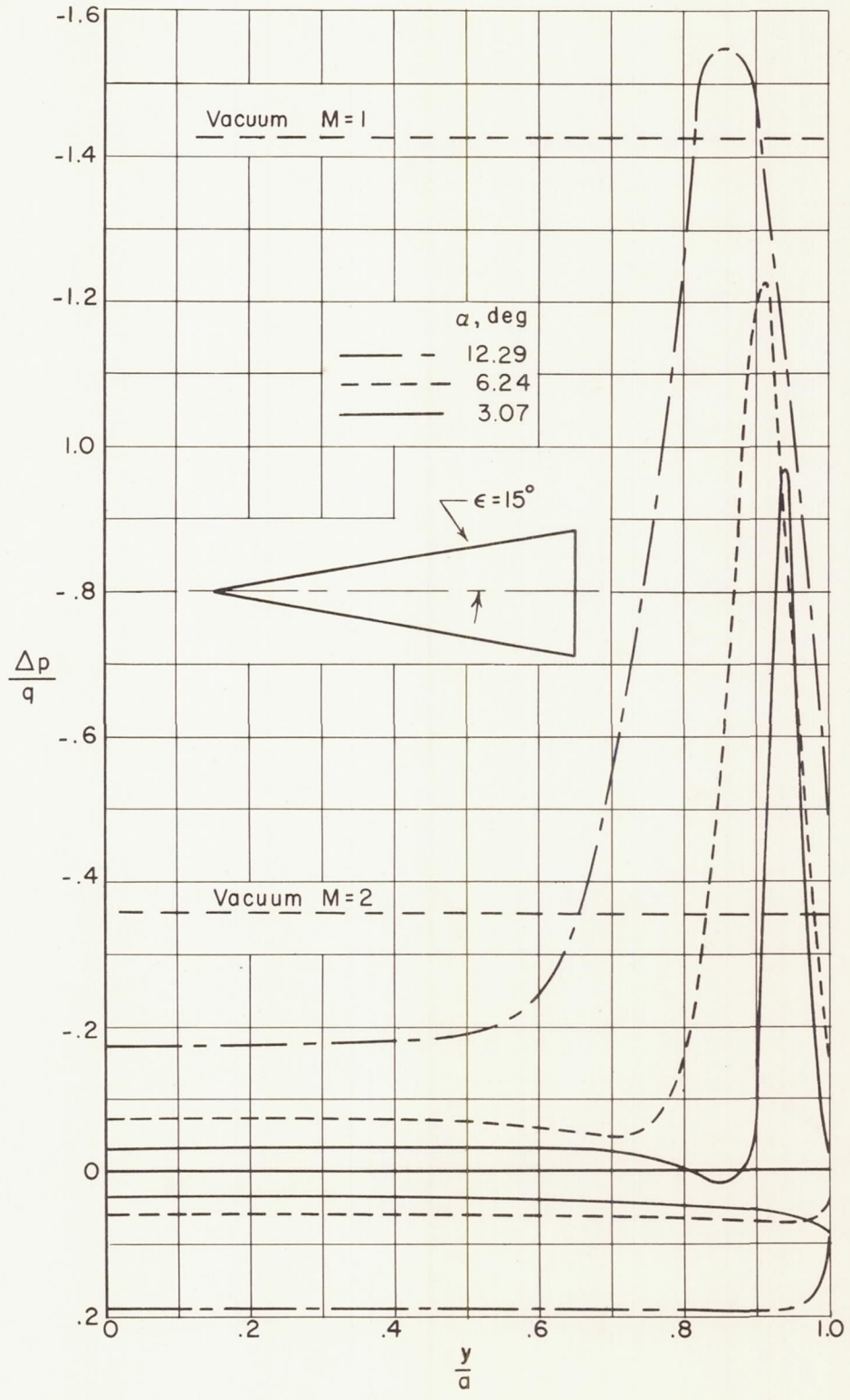

Figure 7.- Pressure distributions.

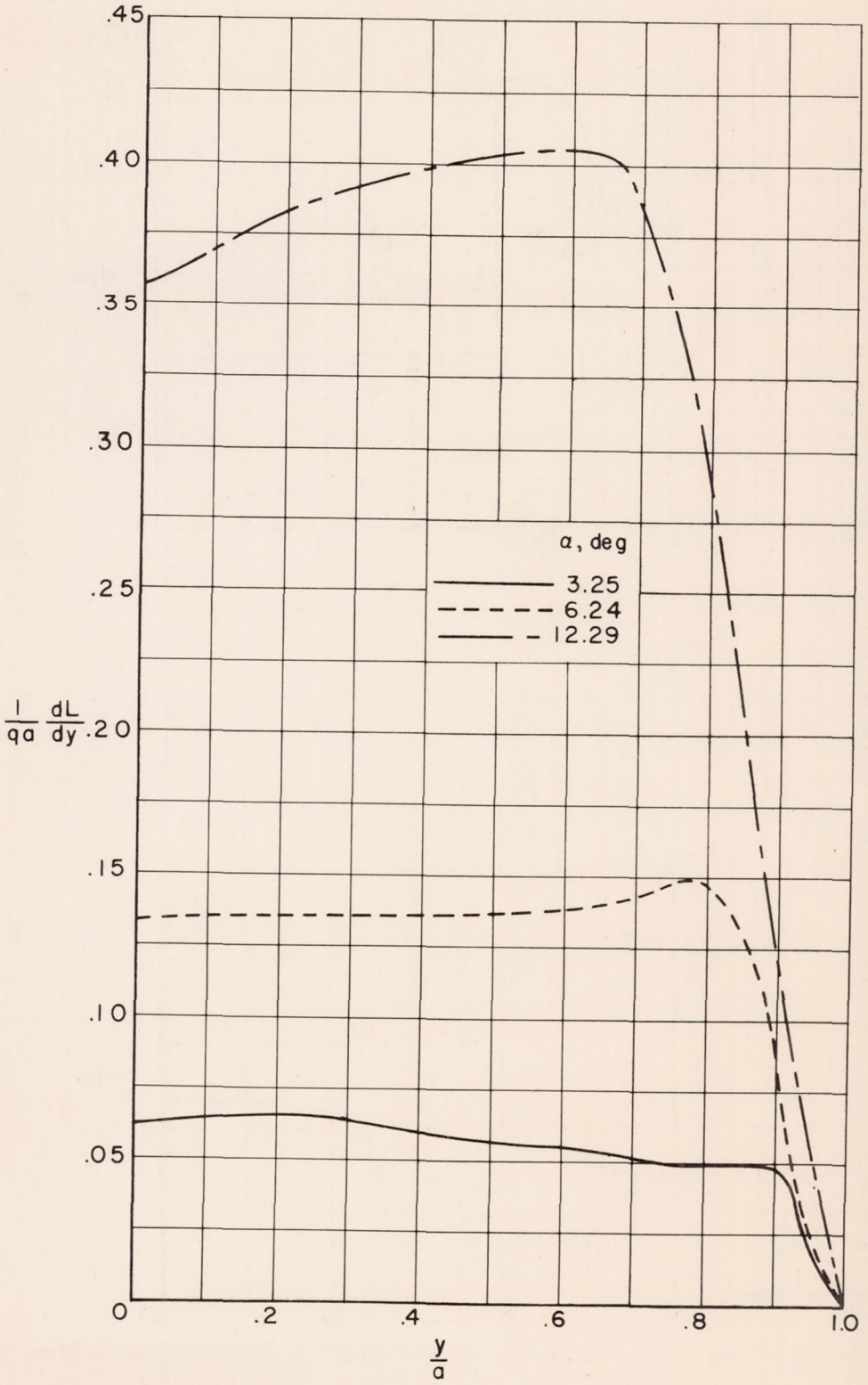

Figure 8.- Spanwise loadings for $\epsilon = 15^{\circ}$.

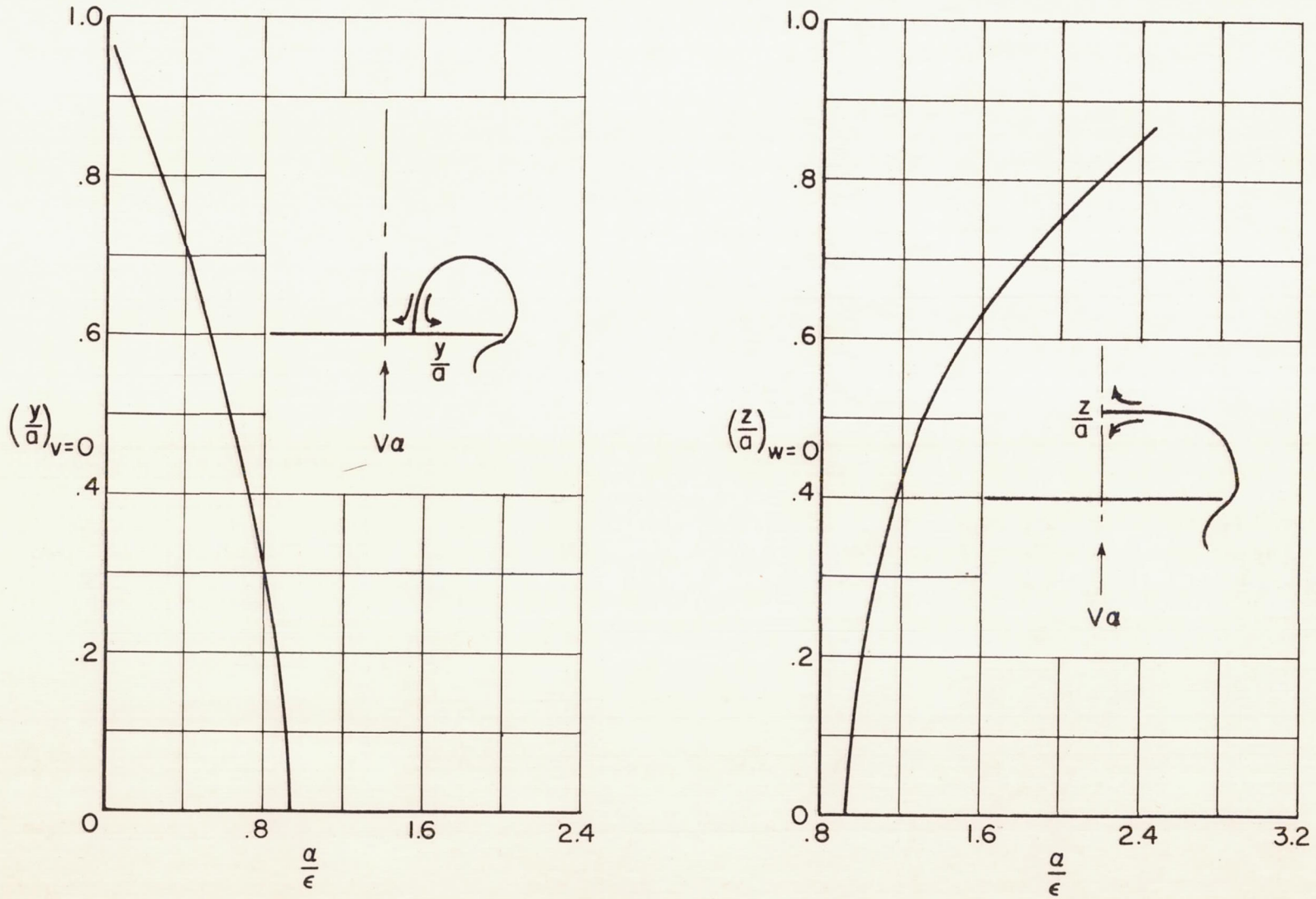

Figure 9.- Stagnation-point locations.

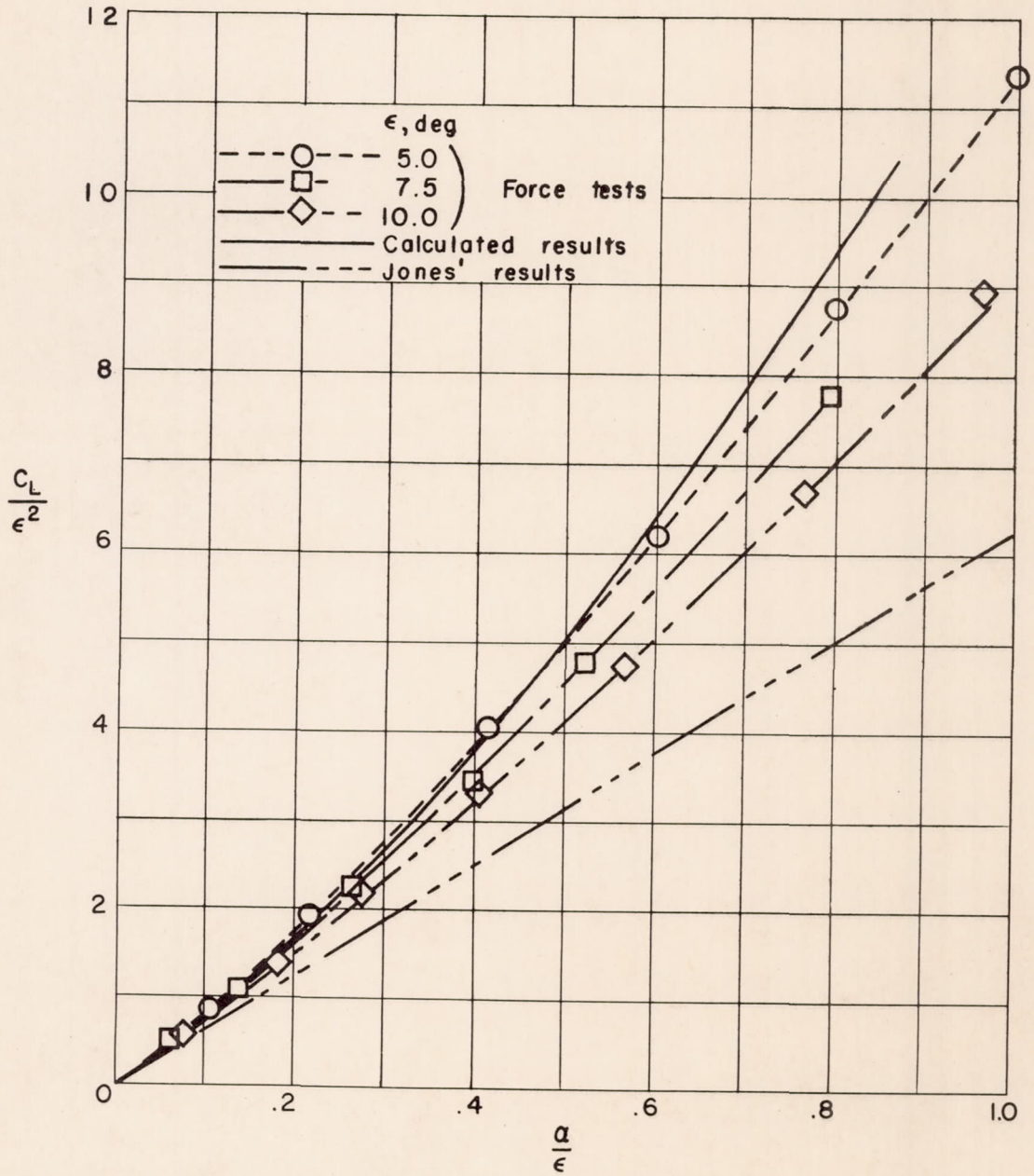

Figure 10.- Comparison of measured and calculated lift results.

NACA-Langley - 4-5-55 - 1000